Magnetotactic bacteria and their mineral inclusions from Hungarian freshwater sediments

Mihály Pósfai and Balázs Arató

Department of Earth and Environmental Sciences

University of Veszprém, Veszprém, POB 158, H8201, Hungary

Submitted to Acta Geologica Hungarica

in revised form on July 24, 2000

Abstract

Magnetotactic bacteria produce nano-scale, intracellular magnetic minerals. The study of such minerals is of interest because it can shed light on biogenic mineral-forming processes, and on the potential contribution of biomagnets to the magnetic signal of sediments and rocks. We collected sediment and water samples from several Hungarian lakes and streams. Magnetotactic bacteria were present in all studied environments; in some samples they occurred in such large numbers that their mineral inclusions likely represent a major source for sediment magnetism. After magnetic enrichment of magnetotactic species, we characterized distinct morphological types using a light microscope. Our systematic study showed that a few bacterium types are widespread in most of the studied freshwater environments.

Using transmission electron microscopy, we studied the composition, microstructure, sizes and habits of magnetite particles from a helicoid magnetotactic bacterium from Gyöngyös stream, Szombathely. Size and shape distributions of the intracellular crystals show some distinct features that may be used for distinguishing bacterial from nonbiogenic magnetite and for identifying possible mechanisms of crystal growth. In particular, the crystal size distribution (CSD) curve is highly asymmetric, consistently with previous observations on magnetite from magnetotactic bacteria. The asymmetry and our new observation of two maxima in the CSD suggest that Ostwald ripening and crystal agglomeration played important roles in the formation of the nano-scale magnetite particles.

Keywords: magnetotactic bacteria, morphological types, BCM, magnetite, crystal size distribution

Introduction

Magnetotactic bacteria grow magnetic minerals (magnetite, Fe_3O_4 or greigite, Fe_3S_4) inside their cells. Since their discovery 25 years ago (Blakemore, 1975), many different types of magnetotactic bacteria were found in diverse aquatic environments (Bazylinski and Moskowitz, 1997); they are widespread in both freshwater and marine environments and in some sediments can be even the dominant species (Spring et al., 1993). Therefore, magnetotactic bacteria may play a significant role in the formation of magnetic iron minerals on a geological scale; however, the importance of the contribution of bacterial minerals to the magnetic remanence of sediments and rocks is unknown.

Magnetotactic bacteria provide a striking example of biologically controlled mineralization (BCM), in which the iron oxide or sulfide crystals within the bacteria grow under a high degree of biological control. The intracellular, nanometer-scale minerals are enclosed by membranes; the ensemble of the crystal and the surrounding membrane is called a magnetosome. It is likely that the growth of intracellular minerals is controlled by this membrane (Gorby et al., 1988), resulting in species or strain-specific sizes and crystal morphologies. In addition, chemical purity and typical microstructural features such as twinning in magnetite (Devouard et al., 1998) and extended defects in greigite (Pósfai et al., 1998) are characteristic of crystals from a certain bacterium strain or species.

Each intracellular crystal comprises a single magnetic domain (Bazylinski and Moskowitz, 1997). These nano-magnets form chains in the cell and are arranged to produce the largest possible magnetic dipole moment, which orients the bacteria parallel to Earth's geomagnetic field lines. Since the field lines are inclined to the surface of the Earth (except at the Equator), this magnetic sensing mechanism helps the bacteria find and maintain an optimal position in the changing chemical environment of their aquatic habitat (Figure 1).

Magnetotactic bacteria or their mineral inclusions have been unknown from Hungarian natural waters and their sediments. We initiated the present study to determine whether magnetotactic bacteria occur and how widespread they seem in distinct freshwater bodies that can be regarded typical environments of current sediment formation. In addition, our goals included the mineralogical study of magnetic crystal inclusions in bacteria from Hungarian lakes and streams. Studies of the sizes, habits, compositions, and microstructural characteristics of iron oxides and sulfides within magnetotactic bacteria are important because they provide information on biogenic mineral-forming processes. The results can be also used to define criteria for identifying bacterial crystals in geological samples, a prerequisite for obtaining a better knowledge about the contributions of biogenic crystals to the magnetic properties of rocks.

In this paper we describe the preliminary results of our collection of magnetotactic bacteria from several lakes and streams, and report on the analysis of magnetite crystals from a magnetotactic species from Gyöngyös stream, Szombathely.

Experimental

We obtained samples from the sediment/water interface simply by filling glass jars or using a sediment sampler where the water was deep. Water depth, temperature, and pH were measured in most cases, and the concentration of dissolved iron was determined in a few cases using a Merck Aquacant rapid test kit (Table 1). Additional samples were collected on an irregular basis; these are also listed in Table 1, even though temperature, pH, or water depth were not measured for them.

We filled glass containers with sediment and water, and enriched magnetotactic bacteria by placing a bar magnet next to the side of the jar, at a level where the aerobic/anaerobic interface was suspected. The bacteria swam to the south pole of the bar magnet (the end that attracts the north-pointing needle of the compass), resulting in their enrichment near the magnet. Water and a little sediment was drawn with a pipette from

next to the magnet, and magnetotactic bacteria were further enriched by attracting them to the tip of the pipette. Thus, the first drop presumably contained most magnetotactic organisms present in the pipette. This drop was placed onto a cover slip and observed as a hanging drop under the optical microscope. A bar magnet was again placed next to the drop, and magnetotactic bacteria could be observed as they were gathering at the edge of the water (Figs. 2a and 2b). When the direction of the magnetic field was changed (by turning the bar magnet), magnetotactic bacteria changed their swimming direction accordingly. This behavior was used to distinguish magnetotactic species from other organisms present in the drop.

Specimens for transmission electron microscopy (TEM) were prepared from drops that contained magnetotactic bacteria by placing the enriched droplets onto holey carbon-coated copper TEM grids. No further specimen treatment was applied. The morphologies of bacteria and their mineral inclusions were studied using a Tesla TEM operated at 80-kV accelerating voltage. We analyzed the compositions of intracellular crystals using energy-dispersive X-ray spectrometry (EDS) in a Philips CM20 TEM operated at 200-kV accelerating voltage and equipped with a Noran Voyager EDS detector. In order to characterize the mineralogical compositions of lake and stream sediments, we obtained standard X-ray powder diffractograms (XRD) from several sediment samples.

Results

Occurrence and morphological types of magnetotactic bacteria

All sediment/water samples that we collected at the end of the summer and early fall of 1999 contained magnetotactic bacteria (Table 1). We included in our exploration a wide variety of natural water bodies, as far as limnological character, temperature, pH, and sediment type are concerned. The list includes the largest lake in Central Europe (Balaton), two major rivers (Tisza, Rába), and several ponds and streams. The temperature ranged from 16.2 °C (where it was measured; Gyöngyös stream was probably

much colder) to 29.6 °C in the outflow of Lake Hévíz (Hévíz Canal) that is fed by hot springs. Calcareous lakes and streams (Balaton, Kornyi, Malom, Hévíz) are neutral or slightly alkaline (with a maximum pH of 8), whereas seasonal ponds on a basaltic plateau (Bonta, Bika, Monostori) are acidic (with pH between 5 and 6). Since we observed magnetotactic bacteria in all samples, and magnetotaxis requires the presence of intracellular magnetic crystals (Frankel and Blakemore, 1989), our observations indicate that magnetic crystals of bacterial origin likely contribute to all studied, currently accumulating freshwater sediments.

Based on size, morphology, speed and mode of swimming, several distinct types of magnetotactic bacteria could be distinguished in the enriched droplets (Table 2). Since these bacteria are wild species and have never been cultured, we know nothing about their metabolism and cell structure. Although we plan to attempt to culture the most common morphological types in the future, the microbiological characterization of the observed bacteria is beyond the scope of this study. The light microscope observations described here are useful for identifying typical morphological types and their occurrences in different samples. Some types occur in several lakes and streams and could even belong to the same species. The characteristic features of these types are given in Table 2, and two examples are shown in Figures 2c and 2d.

The occurrence of distinct morphological types of magnetotactic cells in each sample is listed in the last column of Table 1. The + signs indicate how abundant certain types are under the optical microscope. These observations should be interpreted with caution, because the observed number of bacteria may strongly depend on sampling artifacts; we found that the number of magnetotactic cells is especially sensitive to the depth below the sediment surface from which the enriched droplet is drawn. In addition, in several samples magnetotactic bacteria occur in such large numbers that the abundance of bacteria was judged on the basis of the thickness of the band that accumulated at the edge of the droplet (see the legend to Table 1 and Figures 2a and 2b).

The listings of bacterium types in Table 1 are based on observations performed within a few hours (and at most within two days) after sampling, so the relative abundances of distinct types likely represent the original conditions in the natural environment. We kept the sediment/water samples in the laboratory in capped jars at room temperature, some containers at dimmed light or in the dark, others at natural lighting conditions. Certain bacterium types (the large rods, for example) disappeared from the samples a few days after sampling, whereas others (large cocci, for example) could be observed several months after sampling. Even when the original types survived for a long time, their relative abundances changed; for example, in the Gyöngyös sample large cocci were originally the dominant type, but small spirilla became more abundant four months after sampling.

As far as the distribution of distinct morphological types in different environments is concerned, most bacteria do not seem to be sensitive to temperature and pH. For example, large rods occur in both acidic and alkaline waters, both in lakes and streams, and at every measured temperature. Spirilla are also common in most samples. The only regularity we observed is that great numbers of large cocci occur in relatively cold and clean streams and lakes; in such places they may be even dominant species, particularly in Gyöngyös stream.

Morphologies and size distributions of intracellular magnetite crystals

From the many types of bacteria listed in Table 1, we studied the mineral inclusions in one magnetotactic organism, a bacterium with helicoid morphology from Gyöngyös stream. These bacteria contain chains of magnetite (Fe_3O_4) crystals, such as the one between the arrows in Figure 3a. The mineralogical identity of the crystals was confirmed both by selected-area electron diffraction (SAED) and on the basis of EDS spectra. Apart from Fe, no other transition metals occur in the crystals; C, Ca, Si, and Cl are likely contained in the cell material, whereas the Cu peak is an artifact due to

emission from the Cu specimen support grid (Fig. 4). Typical features other than magnetosomes within the bacteria include dark, round spots (two of them marked by arrows in Figure 3b) that are amorphous and contain mostly P. Such P-containing inclusions are used for the storage of P and are not specific to magnetotactic bacteria.

In bright-field electron micrographs the intracellular magnetite crystals produce strong contrast relative to the rest of the bacterium that contains mostly light elements. Some crystals appear darker than others, owing to diffraction contrast (they are close to a symmetrical zone-axis orientation, resulting in less intensity within the direct beam that was used for forming the image). Some crystals exhibit reentrant angles (such as the one marked by the arrow in Figure 3d), indicating the presence of twin boundaries. It is difficult to obtain an accurate percentage of twinned crystals; likely less than 10% of the total number of magnetite crystals are twinned.

The sizes of magnetite crystals are apparently specific to the particular strain or species we examined. We measured the dimensions of magnetite particles on digitized electron micrographs (such as the ones in Figures 3a and 3b), by fitting ellipses to the outlines of the crystals. The major and minor axes of the best-fitting ellipse were taken as the length and width of the particle, respectively. The same statistical method was used by Devouard et al. (1998) for magnetite crystals from several cultured strains; thus, our results are directly comparable with previous analyses. Since the sizes of crystals were measured in two-dimensional projections, the actual values of length and width could be slightly larger than or equal to the observed ones. A total of 460 crystals were measured to produce the size distributions in Figures 5a and 5b.

The shape of the distribution histogram for the average crystal sizes (Fig. 5a) is consistent with previous results by Meldrum et al. (1993a; 1993b) and Devouard et al. (1998) in that it is quite narrow and shows a distinct asymmetry with a relatively sharp cut-off towards larger sizes. The maximum of the size distribution is between 55 and 70 nm, within the magnetic single-domain range for magnetite. A remarkable feature of the

distribution histogram is a small maximum at 30–35 nm. This maximum at a small particle size is even more prominent when the distributions of length and width values are plotted separately (Fig. 5b).

At low magnification, the magnetite crystals typically look like elongated rectangles in the electron micrographs (Fig. 3). In the literature on magnetotactic bacteria such crystals were often designated “prismatic”, even though this crystal form is incompatible with the cubic system to which magnetite belongs. As discussed by Devouard et al. (1998), the rectangular shapes observed in two-dimensional projections may result from combinations of common cubic forms, such as the cube {100}, the octahedron {111}, and the dodecahedron {110}. In fact, the characteristic angles between octehadral faces can be observed on many crystals (for example, see the third and fourth crystals from the bottom of the chain in Figure 3d). Most crystals are likely elongated octahedra, with [111] oriented parallel to the chain. A statistical analysis of crystal shapes was performed, by taking the width/length value as the shape factor (Fig. 5c). The shape factor histogram has a relatively sharp maximum around 0.85; larger values may represent either real shapes, or result from the fact that even elongated crystals may look isometric in certain projections.

The number of magnetite crystals within individual chains varies from 5 to 28 crystals, as observed in 73 chains (Fig. 5d). When cells divide, the magnetosome chains are probably randomly split, and daughter cells inherit highly variable numbers of magnetite particles.

Discussion

The maxima in the size and shape distributions of magnetite crystals from the studied organism occur at different values than the maxima in similar distributions previously reported for magnetite from magnetotactic bacteria. The marine species MV-1 (Devouard et al., 1998), MV-2 and MV-4 (Meldrum et al., 1993b) produce smaller,

whereas MC-1 (Meldrum et al., 1993a) and MC-2 (Devouard et al., 1998) produce larger crystals than MH-1. (We note that the fact that Meldrum et al. (1993a) used two types of growth media for culturing MC-1 had little effect on the sizes of magnetite crystals.) The extensively studied freshwater species Magnetospirillum magnetotacticum contains magnetite crystals that are smaller than 50 nm (Devouard et al., 1998), and Magnetobacterium bavaricum produces entirely different, bullet-shaped crystals (Hanzlik et al., 1996). MH-1 from Gyöngyös stream is likely a previously undescribed organism.

The number distribution of magnetite crystals within individual chains (Fig. 5d) is also different from those reported previously (Meldrum et al., 1993a; 1993b). When magnetotactic bacteria divide, their magnetosome chain is probably randomly split between the two daughter cells (Bazylinski and Moskowitz, 1997). The maximum in the histogram around 12 crystals is apparently produced by the combined effect of the cell division process and the growth of chains that originally contained less than 12 magnetosomes.

The asymmetric size distribution of magnetite crystals from the studied organism is consistent with earlier reports about the effect of biogenic control on crystal growth. The cut-offs towards larger sizes may indicate that the crystals do not grow further once they reach their species-specific sizes. A mechanism that limits the growth of magnetite crystals may be beneficial to the bacterium because it prevents the magnetosomes from growing into the magnetic two-domain size range, which would reduce the efficiency of its magnetic sensing mechanism. On the basis of model results and a detailed analysis of experimental crystal size distributions, Eberl et al. (1998) found that several crystal growth mechanisms can be distinguished on the basis of crystal size distributions. The shapes of the size distribution histograms in Figures 5a and 5b match those model results of Eberl et al. (1998) that result from Ostwald ripening, during which the relative rate of crystal dissolution and growth is controlled by differences in specific surface area and by diffusion rate. It is possible that several crystals nucleate (typically at the ends of

magnetosome chains), most of which dissolve and only one will grow to the strain-specified size at the expense of the other nuclei. In our electron micrographs there is some evidence that at least two very small crystals occur at the ends of certain magnetosome chains. Another interesting feature in the size distribution curves is the newly observed small maximum at 30–35 nm; the presence of this peak could be explained by crystal agglomeration that is known to produce multimodal size distributions (Eberl et al., 1998). Such agglomeration of growing crystals could also take place at the ends of chains, and may be responsible for the production of twinned crystals.

Although several studies reported that structural perfection is typical of bacterial magnetite, recent investigations showed that BCM magnetite can contain structural irregularities in the form of twins. On the basis of an analysis of crystals from five strains, Devouard et al. (1998) found that the frequency of twinning varied from strain to strain, and up to 40% of the magnetosomes could be twinned. The contact surface between twinned individuals was commonly irregular. Although we did not obtain high-resolution electron micrographs in this study, we could observe twinned crystals from the bacterium from Gyöngyös stream. Typically, the twins appear to have straight boundaries, making their recognition more difficult.

BCM iron minerals are of great interest as potential biomarkers. The morphological similarity of nanometer-scale magnetite and iron sulfides in the Martian meteorite ALH84001 to the same minerals produced by terrestrial magnetotactic bacteria was cited as part of the evidence for ancient life on Mars (McKay et al., 1996). Claims that magnetite particles recovered from modern and ancient sediments are of biological origin have been based on comparisons to similar grains produced by contemporary bacteria (Kirschvink and Chang, 1984; Petersen et al., 1986; Stolz et al., 1986). Therefore, it is of interest whether biogenic and abiogenic magnetite crystals can be distinguished. Since microstructural features such as twinning were found to be common to both bacterial and synthetic magnetite (Devouard, et al., 1998), chemical purity and

narrow size and shape distributions of BCM iron minerals may be the best criteria for identifying bacterial magnetic minerals in sediments and rocks. Although little data exist about the sizes of magnetite crystals produces by inorganic processes, such crystals seem to have size distribution curves showing "tails" extending to large crystal sizes (Devouard et al., 1998). The results of this study confirm that crystal size distributions of magnetite from a certain type of a magnetotactic bacterium have characteristic features that could be used for identifying similar crystals in the geological environment.

It is remarkable that magnetotactic bacteria occurred in every sample we studied, indicating that magnetic minerals are produced in great quantities at the sediment/water interface or within the upper few centimeters of the sediment. We will analyze the mineral inclusions in the other major morphological cell types listed in Table 1 in a similar way as was done in this study. It is unknown whether magnetite magnetosomes within dead bacteria are preserved or dissolved in the sediment as a result of diagenetic redox changes. We plan to address this problem in future studies by determining the depth profile of single-domain, bacterial crystals in sediments where we know that magnetotactic bacteria live at the sediment/water interface. The bacterial origin of the magnetite crystals will be tested by studying their size distributions. Such data are also needed for evaluating the effect of bacterial minerals on sediment magnetism.

Acknowledgements

We thank Dr. Judit Padisák for useful discussions and for help with starting the bacterium sampling. Anita Künsztler, Gizella Rasztovits, and Zsuzsanna Rezner helped to collect samples and analyzed the iron content, and Dr. Katalin Tasnády-Jelinkó provided aid with operating the Tesla TEM. Constructive reviews by Drs. Gyula Szöőr and István Vető improved the manuscript. This research was supported by a grant from the Hungarian Academy of Sciences (AKP #98-94 2.5).

References

Bazylinski, D.A. & Moskowitz, B.M. (1997): Microbial biomineralization of magnetic iron minerals. *In* Banfield, J.F. & Nealson, K.H., (eds.): *Geomicrobiology: Interactions between microbes and minerals*. Washington, D. C.: Mineralogical Society of America, *Reviews in Mineralogy*, **35**:181-223.

Blakemore, R.P. (1975): Magnetotactic bacteria. *Science*, **190**:377-379.

Devouard, B., Pósfai, M., Hua, X., Bazylinski, D.A., Frankel, R.B. & Buseck, P.R. (1998): Magnetite from magnetotactic bacteria: Size distributions and twinning. *Amer. Mineral.*, **83**:1387-1399.

Eberl, D.D., Drits, V.A. & Srodon, J. (1998): Deducing growth mechanisms for minerals from the shape of crystal size distributions. *Amer. J. Science*, **298**:499-533.

Frankel, R.B. & Blakemore, R.P. (1989): Magnetite and magnetotaxis in microorganisms. *Bioelectromagn.*, **10**:223-237.

Gorby, Y.A., Beveridge, T.J. & Blakemore, R.P. (1988): Characterization of the bacterial magnetosome membrane. *J. Bacteriol.*, **170**:834-841.

Hanzlik, M., Winklhofer, M. & Petersen, N. (1996): Spatial arrangement of chains of magnetosomes in magnetotactic bacteria. *Earth. Planet. Sci. Lett.*, **145**:125-134.

Kirschvink, J.L. & Chang, S.-B. (1984): Ultrafine-grained magnetite in deep-sea sediments: possible bacterial magnetofossils. *Geol.*, **12**:559-562.

McKay, D.S., Gibson, E.K., Jr., Thomas-Keprta, K.L., Vali, H., Romanek, C.S., Clemett, S.J., Chillier, X.D.F., Maechling, C.R. & Zare, R.N. (1996): Search for past life on Mars: Possible relic biogenic activity in Martian meteorite ALH84001. *Science*, **273**:924-930.

Meldrum, F.C., Mann, S., Heywood, B.R., Frankel, R.B. & Bazylinski, D.A. (1993a): Electron microscopy study of magnetosomes in a cultured coccoid magnetotactic bacterium. *Proc. Roy. Soc. Lond.*, **B251**:231-236.

Meldrum, F.C., Mann, S., Heywood, B.R., Frankel, R.B. & Bazylinski, D.A. (1993b): Electron microscopy study of magnetosomes in two cultured vibrioid magnetotactic bacteria. *Proc. Roy. Soc. Lond.*, **B251**:237-242.

Petersen, N., Von Dobeneck, T. & Vali, H. (1986): Fossil bacterial magnetite in deep-sea sediments from the South Atlantic Ocean. *Nature*, **320**:611-615.

Pósfai, M., Buseck, P.R., Bazylinski, D.A. & Frankel, R.B. (1998): Reaction sequence of iron sulfides in bacteria and their use as biomarkers. *Science*, **280**:880-883.

Spring, S., Amann, R., Ludwig, W., Schleifer, K.-H., van Gemerden, H. & Petersen, N. (1993): Dominating role of an unusual magnetotactic bacterium in the microaerobic zone of a freshwater sediment. *Appl. Environ. Microbiol.*, **59**:2397-2403.

Stolz, J.F., Chang, S.-B.R. & Kirschvink, J.L. (1986): Magnetotactic bacteria and single-domain magnetite in hemipelagic sediments. *Nature*, **321**:849-851.

Tables

Table 1. Sampling details and morphological types of magnetotactic bacteria as observed with a light microscope

Sampling Location	Sampling Date	Water Temp. (°C)	Water Depth (cm)	pH	Dissolved Fe (mg/l)	Dominant Minerals of the Sediment	Morphological Types of Magnetotactic Bacteria
Balaton, Örvényes	99.09.02.	21.0	150	7	1.2	carbonates	sc+, sp+, lr
Malom-tó, Tapolca	99.08.30.	19.8	80	7	0.8	carbonates	lc++
Kornyi-tó, Kõvágóõrs	99.09.02.	-	60	8	-	carbonates	lr+
Belsõ-tó, Tihany	99.09.02.	22.5	15	8	0.2	-	lr
Külsõ-tó, Tihany	99.09.02.	17.0	10	8	0.8	-	lr, sc
Bonta-tó, Köveskál	99.09.01.	17.4	3	6	10.0	detrital minerals from basalt	ssc
Bika-tó, Köveskál	99.09.01.	16.2	20	5	6.5	detrital minerals from basalt	sc+, lr+
Monostori-tó, Balatonhenye	99.09.01.	16.5	10	6	6.5	-	sp+++, dc+
Fishing Pond, Balatonhenye	99.09.01.	17.0	50	7	0.8	-	lr, lc, ssc,
Pond, Salföld	99.08.30.	19.2	3	7	6.5	quartz	lr, sc+, sp+
Velencei-tó, Pákozd	99.10.11.	-	30	-	-	-	lr+, dc+
Hévíz Canal*, Hévíz	99.08.30.	29.6	100	7	-	carbonates	lr
Tisza*, Szeged	99.09.21.	-	10	-	-	-	lc+, lr+, sc+, sp+
Rába*, Körmend	99.09.29.	-	-	-	-	-	lr+, lc+
Kinizsi-forrás*, Nagyvázsony	99.09.04.	-	20	-	-	-	lc++
Gerence*, Takácsi	99.09.11.	17.1	-	5	-	-	lc+++, sp
Marcal*, Mersevát	99.09.12.	18.5	-	5	-	-	lc+++
Répce*, Csánig	99.09.12.	18.0	-	7	-	-	lc+++
Bakonyér*, Gyõrszemere	99.09.11.	23.1	-	7	-	-	lc+++
Gyöngyös*, Szombathely	99.10.10.	-	15	-	-	detrital minerals from metamorphic rocks	lc++++, sp

*: rivers and streams; the other items are ponds and lakes;
sc: small coccus; sp: spirillum; lr: large rod; lc: large coccus; dc: diplococcus; ssc: small slow coccus;
+ signs indicate relative abundances (no sign: only a few cells; +: up to ~100 cells; ++: continuous band of bacteria at the edge of the drop; +++: several μm wide, continuous band of bacteria at the edge of the drop; ++++: >10-μm wide, continuous band of bacteria at the edge of the drop)

Table 2. Morphological types and optically visible characteristics of observed magnetotactic bacteria

Type	Characteristic features
large rod	5–10 μm long, slow-moving rods; contain dark spots
large coccus	2–5 μm large, very fast-swimming cocci; contain high-contrast spots
small coccus	< 2 μm, fast-swimming cocci
small slow coccus	< 2 μm, very slow-swimming cocci
spirillum	1–2 μm long spirilla
diplococcus	2–5 μm large diplococci

Figure Captions

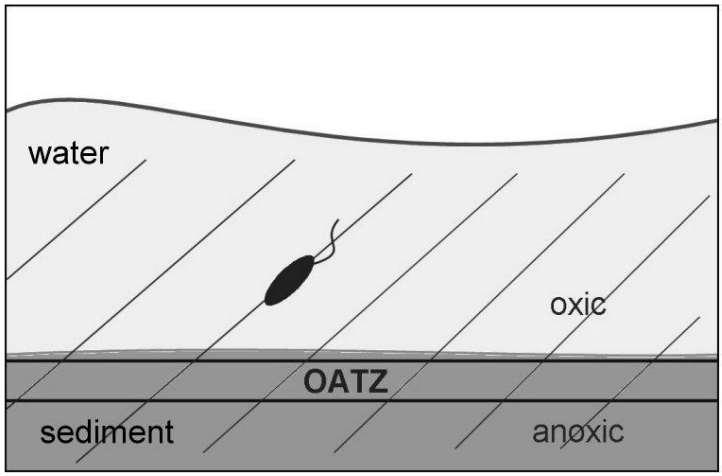

Fig. 1.
Pósfai and Arató: Magnetotactic bacteria...

Fig. 1. A schematic representation of the use of magnetic sensing in magnetotactic bacteria. The bacterium is aligned by the Earth's magnetic field and can swim only along the magnetic field lines; thus, it does not have to search for the "up" and "down" direction, but easily finds its optimal chemical environment within the OATZ (Oxic-Anoxic Transition Zone).

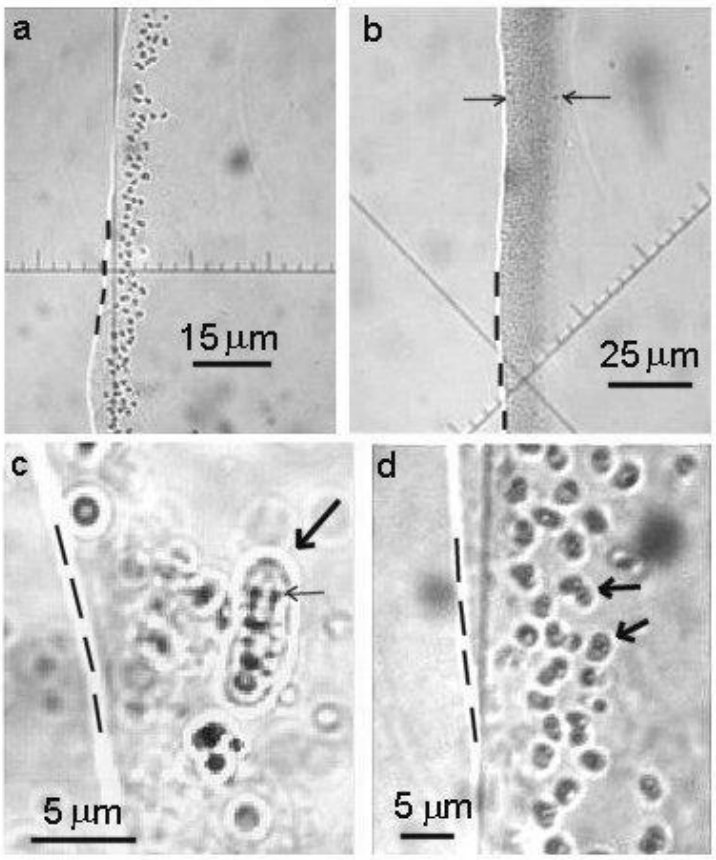

Fig. 2.
Pósfai and Arató: Magnetotactic bacteria...

Fig. 2. Light microscope images of live magnetotactic bacteria. The nearly vertical white line in all four images (partly marked by the broken line) is the edge of the droplet (water is always to the right of the boundary line). (a) A continuous band of cocci at the edge of the drop (Malom-tó, Tapolca); such abundances are marked ++ in Table 1. (b) A thick band of magnetotactic bacteria from Marcal (between the two arrows) gathering at the drop edge; similar abundances are marked +++ in Table 1. (c) A large rod (marked by the thick arrow) from Kornyi-tó; the small arrow points to high-contrast features within the cell. (d) Large cocci (two of them arrowed) with dark-contrast spots (Malom-tó, Tapolca).

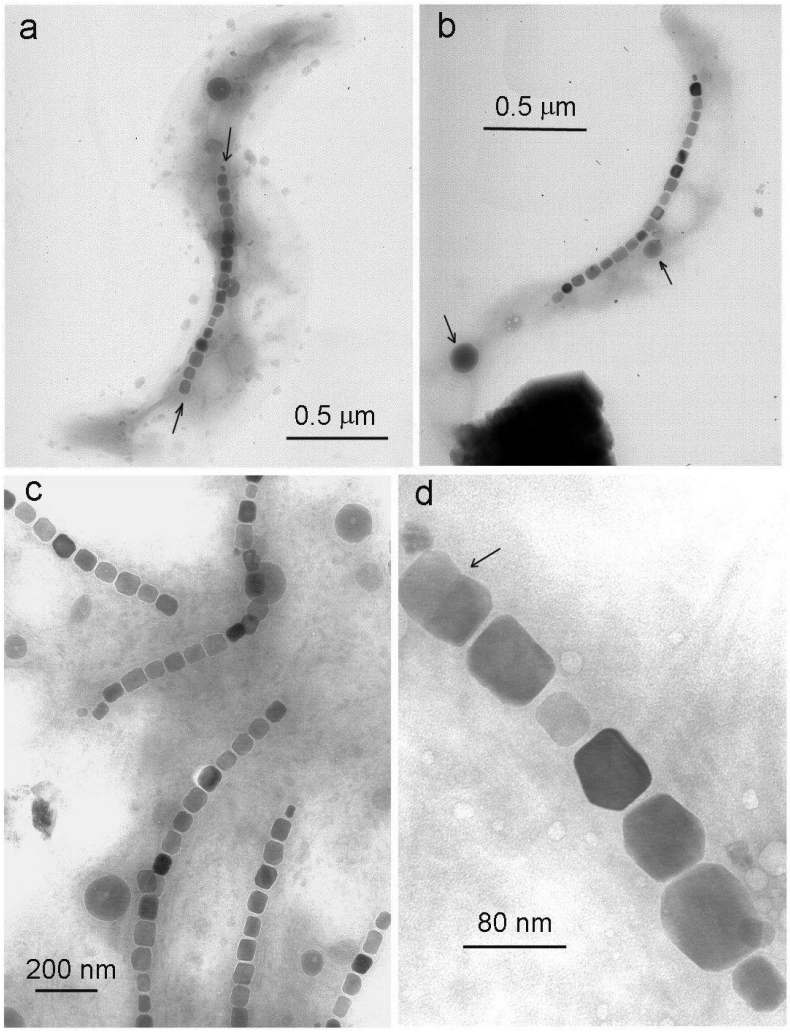

Fig. 3.
Pósfai and Arató: Magnetotactic bacteria...

Fig. 3. Bright-field transmission electron microscope images of chains of magnetite crystals in helicoid bacteria from Gyöngyös stream, Szombathely. Individual bacteria are shown in (a) and (b), whereas several bacteria are aggregated in (c); part of a chain is shown at higher magnification in (d). The arrows mark the magnetite chain in (a), P-containing spots in (b), and a twinned crystal in (d).

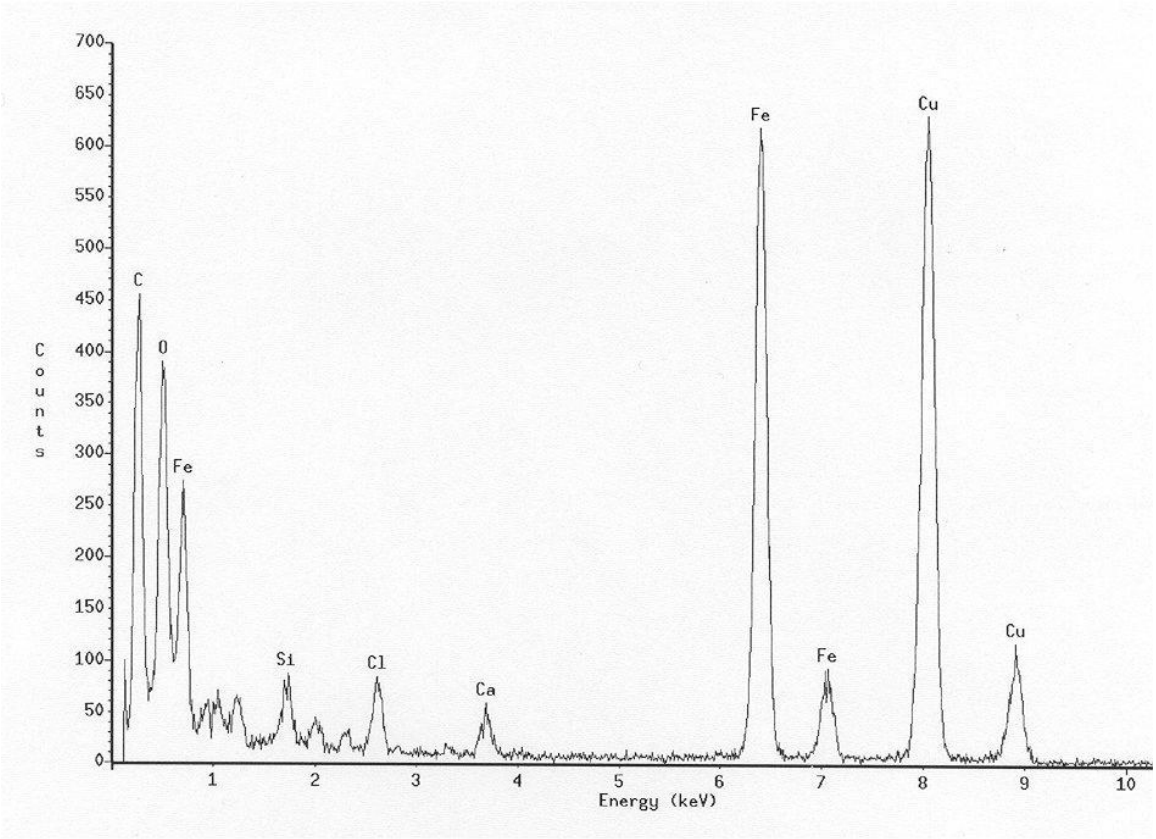

Fig. 4.
Pósfai and Arató: Magnetotactic bacteria...

Fig. 4. A representative energy-dispersive X-ray spectrum obtained from one magnetite crystal (see text for details).

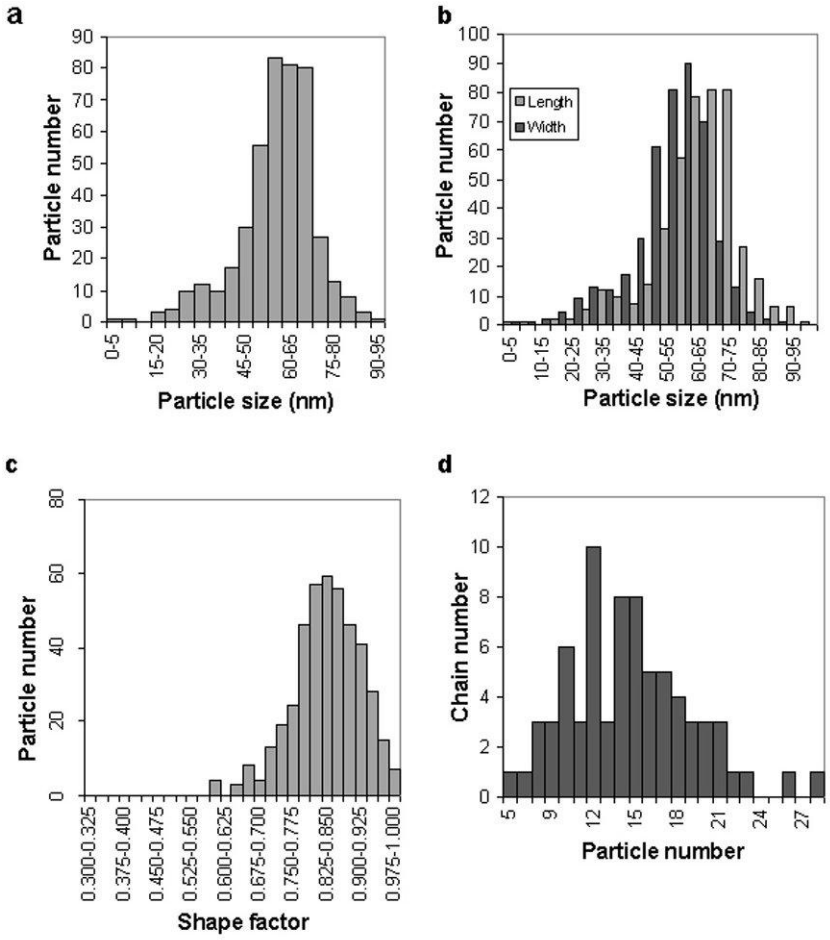

Fig. 5.
Pósfai and Arató: Magnetotactic bacteria...

Fig. 5. (a) and (b) Size distribution histograms of magnetite crystals from a helicoid bacterium from Gyöngyös stream. Average particle sizes [(length + width)/2] are shown in (a), whereas the distributions of width and length values are given in (b). (c) Shape distribution of magnetite particles (shape factor = width/length). (d) Distribution of the number of magnetite particles in individual chains of magnetosomes.